



This is a repository copy of *Low-noise AlGaAsSb avalanche photodiodes for 1550nm light detection*.

White Rose Research Online URL for this paper:

<https://eprints.whiterose.ac.uk/197832/>

Version: Published Version

---

**Proceedings Paper:**

Collins, X., White, B., Cao, Y. [orcid.org/0000-0002-6353-7660](https://orcid.org/0000-0002-6353-7660) et al. (4 more authors) (2022) Low-noise AlGaAsSb avalanche photodiodes for 1550nm light detection. In: Jiang, S. and Digonnet, M.J.F., (eds.) Optical Components and Materials XIX. Optical Components and Materials XIX, 22 Jan - 28 Feb 2022, San Francisco, California, United States. Proceedings of SPIE, 11997 . Society of Photo-optical Instrumentation Engineers (SPIE) , p. 1199709. ISBN 9781510648654

<https://doi.org/10.1117/12.2608842>

---

Xiao Collins, Benjamin White, Ye Cao, Tarick Osman, Jonathan Taylor-Mew, Jo Shien Ng, Chee Hing Tan, "Low-noise AlGaAsSb avalanche photodiodes for 1550nm light detection," Proc. SPIE 11997, Optical Components and Materials XIX, 1199709 (4 March 2022); <https://doi.org/10.1117/12.2608842> © 2022 Society of Photo Optical Instrumentation Engineers (SPIE). One print or electronic copy may be made for personal use only. Systematic reproduction and distribution, duplication of any material in this publication for a fee or for commercial purposes, or modification of the contents of the publication are prohibited.

**Reuse**

Items deposited in White Rose Research Online are protected by copyright, with all rights reserved unless indicated otherwise. They may be downloaded and/or printed for private study, or other acts as permitted by national copyright laws. The publisher or other rights holders may allow further reproduction and re-use of the full text version. This is indicated by the licence information on the White Rose Research Online record for the item.

**Takedown**

If you consider content in White Rose Research Online to be in breach of UK law, please notify us by emailing [eprints@whiterose.ac.uk](mailto:eprints@whiterose.ac.uk) including the URL of the record and the reason for the withdrawal request.



[eprints@whiterose.ac.uk](mailto:eprints@whiterose.ac.uk)  
<https://eprints.whiterose.ac.uk/>

# PROCEEDINGS OF SPIE

[SPIDigitalLibrary.org/conference-proceedings-of-spie](https://SPIDigitalLibrary.org/conference-proceedings-of-spie)

## Low-noise AlGaAsSb avalanche photodiodes for 1550nm light detection

Xiao Collins, Benjamin White, Ye Cao, Tarick Osman, Jonathan Taylor-Mew, et al.

Xiao Collins, Benjamin White, Ye Cao, Tarick Osman, Jonathan Taylor-Mew, Jo Shien Ng, Chee Hing Tan, "Low-noise AlGaAsSb avalanche photodiodes for 1550nm light detection," Proc. SPIE 11997, Optical Components and Materials XIX, 1199709 (4 March 2022); doi: 10.1117/12.2608842

**SPIE.**

Event: SPIE OPTO, 2022, San Francisco, California, United States

# Low-noise AlGaAsSb avalanche photodiodes for 1550 nm light detection

Xiao Collins\*<sup>a</sup>, Benjamin White <sup>a</sup>, Ye Cao<sup>b</sup>, Tarick Osman<sup>b</sup>, Jonathan Taylor-Mew<sup>b</sup>, Jo Shien Ng<sup>b</sup>  
and Chee Hing Tan<sup>b</sup>

<sup>a</sup>Phlux Technology Ltd, The Innovation Centre, 217 Portobello, Sheffield  
S1 4DP UK; <sup>b</sup> Department of Electronic and Electrical Engineering, University of Sheffield, Mappin  
Street, Sheffield S1 3JD, United Kingdom

## ABSTRACT (250 WORDS)

The optical detector used in pulsed LIDAR, range finding and optical time domain reflectometry systems is typically the limiting factor in the system's sensitivity. It is well-known that an avalanche photodiode (APD) can be used to improve the signal to noise ratio over a PIN detector, however, APDs operating at the eye-safe wavelengths around 1550 nm are limited in sensitivity by high excess noise. The underlying issue is that the impact ionization coefficient of InAlAs and InP used as the avalanche region in current commercial APDs are very similar at high gain, leading to poor excess noise performance. Recently, we have demonstrated extremely low noise from an Al(Ga)AsSb PIN diode with highly dissimilar impact ionization coefficients due to electron dominated impact ionization.

In this paper, we report on the first low noise InGaAs/AlGaAsSb separate absorption, grading and multiplication APDs operating at 1550 nm with extremely low excess noise factor of 1.93 at a gain of 10 and 2.94 at a gain of 20. Furthermore, the APD's dark current density was measured to be 74.6  $\mu\text{A}/\text{cm}^2$  at a gain of 10 which is competitive with commercial devices. We discuss the impact of the excess noise, dark current and responsivity on the APDs sensitivity and, project a noise-equivalent power (NEP) below 80 fW/Hz<sup>0.5</sup> from a 230  $\mu\text{m}$  diameter APD and commercial transimpedance amplifier (TIA). The prospects for the next generation of extremely low noise APDs for 1550 nm light detection are discussed.

**Keywords (8):** AlGaAsSb, avalanche photodiode, excess noise, photodetector, NIR, LIDAR, impact ionization

## 1. INTRODUCTION

Avalanche photodiodes (APDs) have been known to improve the signal to noise ratio of optical receivers compared to unity gain PIN detectors and thus are widely used in LIDAR, range finding and optical time domain reflectometry. For high sensitivity at weak optical signals, the excess noise factor (F) of the APD is a critical factor in determining the system sensitivity. Current APDs operating at eye-safe wavelengths as around 1550 nm are typically comprised of InGaAs/InAlAs and InGaAs/InP using a separate absorption and multiplication (SAM) APD structure. The avalanche materials typically used in these SAM APDs, InAlAs<sup>1</sup> and InP<sup>2</sup>, have very similar electron ( $\alpha$ ) and hole ( $\beta$ ) impact ionization coefficients, and thus an impact ionization coefficient ratio ( $k = \beta/\alpha$ ) close to unity. As demonstrated in equation 1, this results in an excess noise factor which tends towards M when  $\alpha = \beta$  limiting the APDs useful gain to values of 10 to 20.

$$F = kM + (1 - k) \left( 2 - \frac{1}{M} \right) \quad (1)$$

More recently there have been reports of extremely low multiplication noise using materials such as Al<sub>0.85</sub>Ga<sub>0.15</sub>As<sub>0.56</sub>Sb<sub>0.44</sub> (hereafter referred to as AlGaAsSb)<sup>3</sup>, AlAsSb<sup>4</sup>, and AlInAsSb<sup>5</sup> (on GaSb). These materials promise to bring new levels of sensitivity to detectors operating in the eye-safe infrared region. Of these materials, AlGaAsSb is perhaps the most promising candidate for low noise APDs operating at 1550 nm as it can also be lattice matched to InP substrates. AlGaAsSb SAM APDs can therefore make use of high-quality InGaAs absorbers, and such structures are compatible with established manufacturing processes for InP.

Phlux Technology presents the first demonstration of a low noise SAM APD operating at 1550 nm with a AlGaAsSb multiplication region to achieve extremely low noise, low dark current and high sensitivity.

## 2. EXPERIMENTAL DETAILS

The SAM APD wafer was grown by molecular beam epitaxy on a semi-insulating InP substrate. The epi structure of the APDs is shown in figure 1a and comprises of an InGaAs absorption layer and an AlGaAsSb multiplication layer. A field control layer was grown to increase the electric field and a grading layer to aid carrier transport. Circular mesa diodes of radii between 60 and 230  $\mu\text{m}$  were fabricated using a wet etching process. Ti/Au metal contacts were evaporated onto InGaAs contact layers to form Ohmic contacts before the devices were passivated to allow for remote bond pads to be placed for wire ball bonding. Finally, devices were cleaved into individual die of area 500 x 500  $\mu\text{m}$  for packaging onto a ceramic sub-mount as shown in figure 1b.

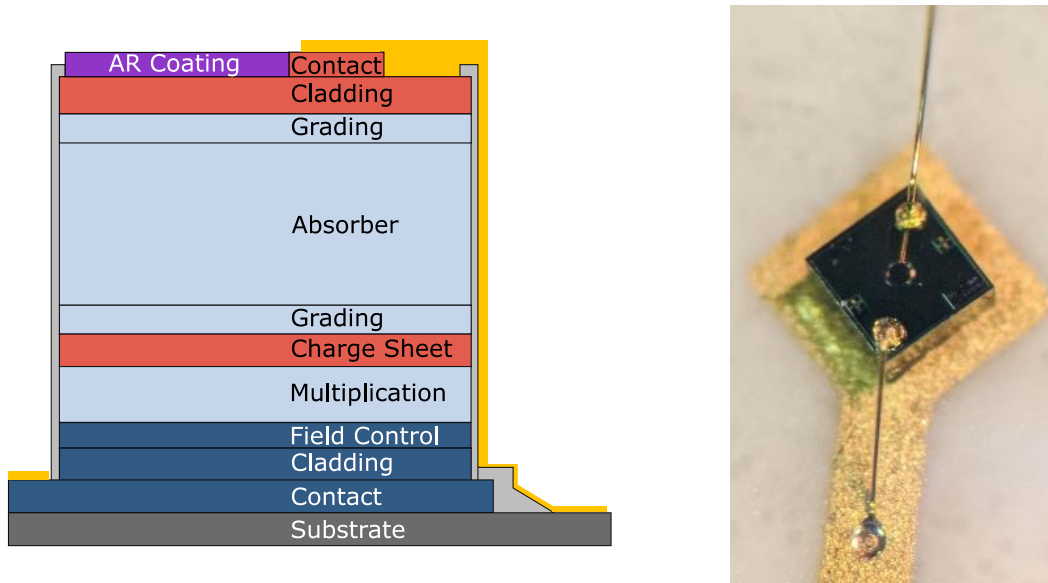


Figure 1. (a) A schematic diagram of the layer structure of the APD (b) An image showing a single APD die bonded onto a ceramic header. The optically active part of the APD is an 80  $\mu\text{m}$ -diameter window in the center of the die.

Gain measurements were performed using phase-sensitive techniques using a lock-in amplifier and chopped He-Ne laser at 1550 nm and modulated LED at 940 nm. The gain was verified to be the same for both 940 nm and 1550 nm, which is expected as both 940 nm and 1550 nm are solely absorbed in the InGaAs absorber, providing pure carrier injection into the AlGaAsSb multiplication region.

Unity gain and responsivity of the APDs were validated against a reference photodiode with the same absorption layer thickness. Responsivity and gain results were also corroborated against the theoretical value for responsivity which was calculated using the absorption coefficient of InGaAs<sup>6</sup> and accounting for reflections from the optical window.

Excess noise measurements as a function of gain (F(M)) were carried out by phase-sensitive detection and a modulated 940 nm LED. The experimental setup is described elsewhere in further detail<sup>7</sup>.

## 3. RESULTS

The room temperature IV characteristics of a device with diameter of 230  $\mu\text{m}$  are shown in figure 2. The device has a punchthrough voltage of -24V and a breakdown voltage of -50V. No edge breakdown was found in the devices, and the magnitude of the dark current was established to be consistent over many devices of varying sizes.

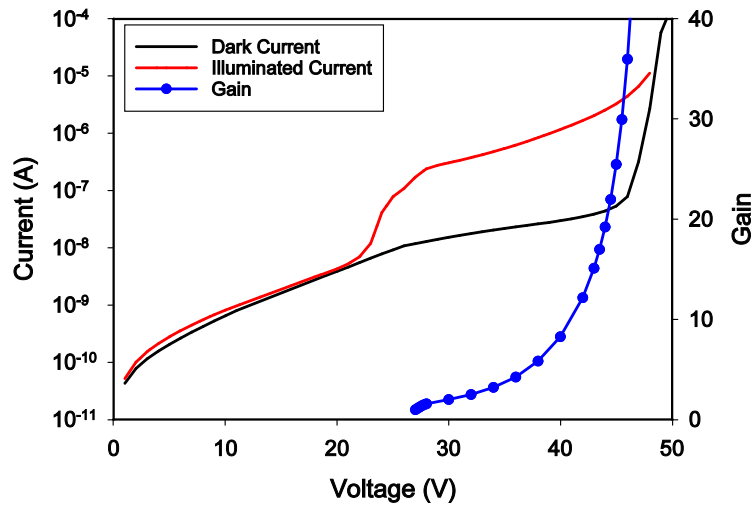


Figure 2. Room temperature dark current (black, left axis), photocurrent (red, left axis) and avalanche gain (blue, right axis) versus reverse voltage for the InGaAs/AlGaAsSb SAM APD. The device used is a 230  $\mu\text{m}$  diameter circular mesa. Gain is calculated by dividing the responsivity by the unity gain responsivity.

The 230  $\mu\text{m}$  diameter APDs had an average dark current of 31 nA at a gain of 10, equivalent to a current density of 74.6  $\mu\text{Acm}^{-2}$ . To investigate the source of the leakage current, the unmultiplied ( $I_{\text{surface}}$ ) and multiplied ( $I_{\text{bulk}}$ ) components of the dark current were calculated. Typically, the unmultiplied component of the leakage is due to surface effects and the multiplied is due to bulk related leakage current usually stemming from the low band gap material.  $I_{\text{surface}}$  and  $I_{\text{bulk}}$  were calculated by fitting the two components across a range of voltages using a linear regression between dark current and gain using equation 2.<sup>8</sup> The unmultiplied and multiplied dark currents of the 230  $\mu\text{m}$  diameter APD were found to be 18 nA and 1.3 nA respectively over a voltage range of 36 to 44V corresponding to gain values of 3.5 to 20.

$$I = I_{\text{surface}} + I_{\text{bulk}}M \quad (2)$$

We find that the total dark current is dominated by surface current at voltages less than 45 V and bulk current at > 45V. The 230  $\mu\text{m}$  diameter APD allows for a circular optical window of diameter 200  $\mu\text{m}$ , the bulk dark current can be compared to mature commercial InGaAs APDs also with an optical window of 200  $\mu\text{m}$ . At a gain of 10, the bulk dark current of the AlGaAsSb APDs is just 13 nA, which is comparable to mature commercial InGaAs APDs by Hamamatsu (20 nA)<sup>9</sup>, Excelitas (45 nA)<sup>10</sup> and Laser Components (25 nA)<sup>11</sup>. The dark current of the AlGaAsSb APDs reported here is also much lower than reports of low noise AlInAsSb SAM APDs (6.1  $\text{mAcm}^{-2}$ ) using an  $\text{Al}_{0.4}\text{In}_{0.6}\text{As}_{0.3}\text{Sb}_{0.7}$  absorber<sup>5</sup>. This result demonstrates the potential for low dark current AlGaAsSb APDs, which is a key metric in determining NEP. A detailed analysis of the dark current leakage mechanisms is underway and will be the subject of a further study.

The device was illuminated by a 1550 nm continuous wave laser with a power of 180 nW for the illuminated IV, and the responsivity at punchthrough is 0.79 A/W by utilizing a SiN anti-reflection coating (ARC). The gain of the APD was found to be 1.05 at punch through.

APDs with low capacitance are highly desirable to reduce the TIA amplifier noise, gain peaking and improve the TIA amplifier's stability. The InGaAs/AlGaAsSb APD of this study has a capacitance density of just 6.7  $\text{nFcm}^{-2}$ , which is 2.8 pF for a device with a 230  $\mu\text{m}$  diameter.

### 3.1 Excess Noise

The excess noise factor of the InGaAs/AlGaAsSb APD is shown in figure 3 and is the average of 10 different devices. Reference lines for the theoretical excess noise of APDs with varying k-values calculated using McIntyre's local model,

and the expected excess noise performance of typical APDs that use InAlAs<sup>8,12</sup> or InP<sup>13</sup> as the avalanche layer are also shown for comparison.

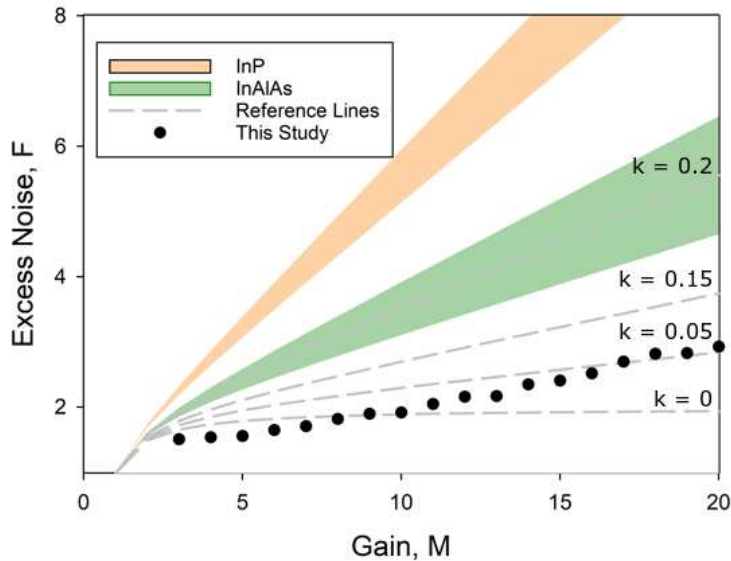


Figure 3. The excess noise factor of the AlGaAsSb APDs along with reference lines depicting the excess noise predicted by equation 1 for values of  $k$  between 0 and 0.2. Typical values for InP<sup>13</sup> and InAlAs<sup>8,12</sup> are also added on the figure in orange and green respectively.

The excess noise factor of the AlGaAsSb SAM APD was found to be 1.93 at a gain of 10 and 2.93 at 20. This is a significantly lower than the excess noise of widely available InAlAs and InP APDs and was achieved using a careful optimization of the electric field profile and avalanche region in a SAM APD structure. The low excess noise of the InGaAs/AlGaAsSb APDs enables the APD to be operated at a much higher gain than InAlAs and InP APDs before the signal to noise ratio begins to deteriorate.

The effect of the low excess noise factor and low dark current of AlGaAsSb can be demonstrated by calculating the noise-equivalent power, given by

$$NEP = \frac{1}{R} \left( \sqrt{2q(I_{surface} + I_{bulk}M^2F) + n_{amp}^2} \right), \quad (3)$$

where  $R$  is the responsivity and  $n_{amp}$  is the noise spectral density of an external amplifier. Other sources of noise such as thermal and  $1/f$  have been ignored as the noise currents due to APD and external amplifier are expected to be dominant.

Without the effect of the amplifier, figure 4a shows the difference between the NEP calculated using the responsivity and dark current of the AlGaAsSb APD and NEP values obtained from commercial datasheets of APDs for 1550 nm detection. The NEP of the AlGaAsSb APDs was calculated using a unity gain responsivity = 0.78 A/W, the dark current as fitted using equation 2 and the excess noise factor from figure 3. All values are stated at a gain of 10. Due to the low multiplied dark current and low excess noise factor, the NEP of the AlGaAsSb APDs is lower than that for InAlAs and InP commercial APDs of the same sized devices.

The NEP of our InGaAs/AlGaAsSb SAM APD is compared to theoretical APDs with various  $k$ -values in figure 4b. The  $k$  values for the green and orange line are significant as they represent the typical  $k$ -value for InAlAs and InP APDs respectively. Therefore, they represent the limitations of those materials to reach the same NEP given the same dark current and responsivity as the InGaAs/AlGaAsSb APD of this study. The amplifier noise used to calculate the NEP is  $n_{amp} =$

$1 \times 10^{-12} \text{ A/Hz}^{0.5}$ , as well as the responsivity, dark current and excess noise previously stated. The effect of the low excess factor can be observed for  $M = 20$ , where the noise contribution from the APD becomes the dominant component of equation 3, and any further increase in APD gain degrades the system signal to noise ratio. The NEP is much lower for the AlGaAsSb APDs compared to theoretical lines for InAlAs or InP due to the excess noise factor. We expect the NEP of future devices to follow a trend closer to the red dashed line where the multiplied dark current has been decreased further to  $1 \text{ nA}$  and the responsivity increased to  $0.9 \text{ A/W}$ . With these parameters, the NEP is found to continue to improve with increasing gain reaching a minimum of  $36 \text{ fW/Hz}^{0.5}$  for a  $230 \mu\text{m}$  APD at  $M = 70$ . Therefore, in the future we are aiming to measure the excess noise factor and NEP at a much higher gain which is achievable with AlGaAsSb APDs.

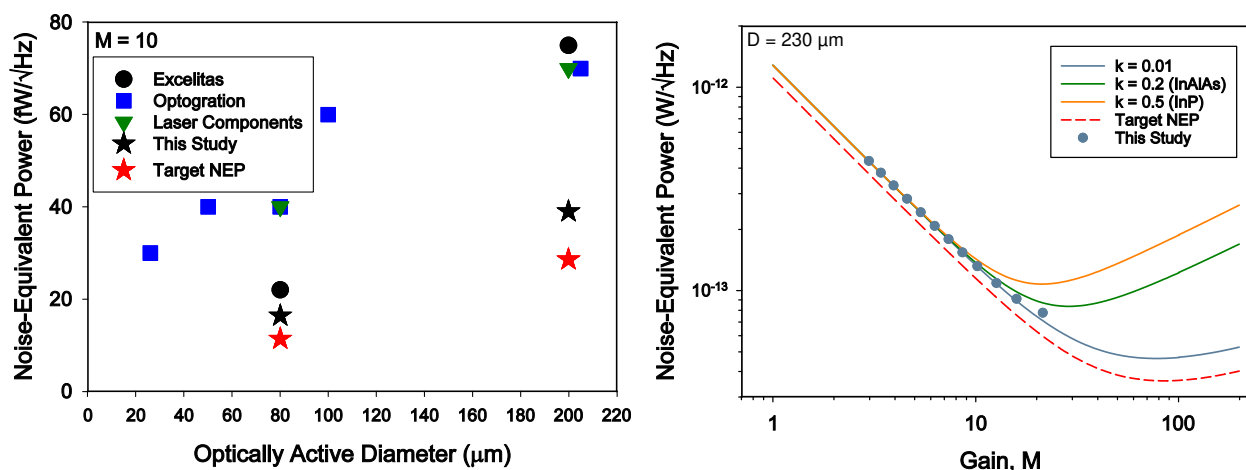


Figure 4 (a) The NEP of the AlGaAsSb APD compared with commercial InAlAs and InP APDs.<sup>10,11,14</sup> (b) The NEP of the AlGaAsSb APD of this study (symbols) and the NEP of theoretical APDs with constant  $k$  values (lines) as calculated by equation 3 including the effect of amplifier noise. The green and orange lines indicate the expected  $k$  values for InAlAs and InP APDs respectively.

#### 4. CONCLUSION

At Phlux Technology we have designed and fabricated InGaAs/AlGaAsSb SAM APD for visible to short-wavelength infrared applications such as LIDAR and range finding. We demonstrate AlGaAsSb APDs with extremely low excess noise factors of 1.93 and 2.94 at gains of 10 and 20 respectively, representing a great improvement over InAlAs and InP based APDs. The dark current of an APD with diameter  $230 \mu\text{m}$  is  $31 \text{ nA}$  at a gain of 10. This dark current is mostly caused by surface-related dark current rather than bulk-related dark current which is multiplied and significantly contributes to the noise current generated by the APD. This work demonstrates the potential for Phlux’s AlGaAsSb based APDs for high performance sensing around  $1550 \text{ nm}$ .

Further improvements to the APD are on the horizon. These will reduce the dark current and achieve even lower noise at higher gains, performance which is unachievable in InAlAs and InP APDs since these materials are fundamentally limited by the ratio of impact ionization coefficients.

#### REFERENCES

- [1] Goh, Y. L., Massey, D. J., Marshall, A. R. J., Ng, J. S., Tan, C. H., Ng, W. K., Rees, G. J., Hopkinson, M., David, J. P. R. and Jones, S. K., “Avalanche multiplication in InAlAs,” *IEEE Trans. Electron Devices* **54**(1), 11 (2007).

- [2] Tan, L. J. J., Ng, J. S., Tan, C. H. and David, J. P. R., “Avalanche noise characteristics in submicron InP diodes,” *IEEE J. Quantum Electron.* **44**(4), 378–382 (2008).
- [3] Taylor-Mew, J., Shulyak, V., White, B., Tan, C. H. and Ng, J. S., “Low Excess Noise of Al<sub>0.85</sub>Ga<sub>0.15</sub>As<sub>0.56</sub>Sb<sub>0.44</sub> Avalanche Photodiode From Pure Electron Injection,” *IEEE Photonics Technol. Lett.* **33**(20), 1155–1158 (2021).
- [4] Tan, C. H., Xie, S. and Xie, J., “Low noise avalanche photodiodes incorporating a 40 nm ALASSB avalanche region,” *IEEE J. Quantum Electron.* **48**(1), 36–41 (2012).
- [5] Bank, S. R., Campbell, J. C., Maddox, S. J., Ren, M., Rockwell, A., Woodson, M. E. and March, S. D., “Avalanche Photodiodes Based on the AlInAsSb Materials System,” *IEEE J. Sel. Top. Quantum Electron.* **24**(2) (2018).
- [6] Adachi, S., [Physical Properties of III-V Semiconductor compounds], John Wiley and Sons (1992).
- [7] Taylor-Mew, J., Shulyak, V., White, B., Tan, C. H. and Ng, J. S., “Low Excess Noise of Al<sub>0.85</sub>Ga<sub>0.15</sub>As<sub>0.56</sub>Sb<sub>0.44</sub> Avalanche Photodiode From Pure Electron Injection,” *IEEE Photonics Technol. Lett.* **33**(20), 1155–1158 (2021).
- [8] Lahrichi, M., Glastre, G., Derouin, E., Carpentier, D., Lagay, N., Decobert, J. and Achouche, M., “240-GHz Gain-Bandwidth Product Back-Side Illuminated AlInAs Avalanche Photodiodes,” *IEEE Photonics Technol. Lett.* **22**(18), 1373–1375 (2010).
- [9] “Hamamatsu G14858-0020AA APD.”, <<https://www.hamamatsu.com/us/en/product/type/G14858-0020AA/index.html>> (25 January 2022 ).
- [10] “Excelitas C30645 and C30662 APD.”, <<http://www.amstechnologies-webshop.com/media/pdf/e8/92/fe/C30645-C30662-Series-InGaAs-APD-Excelitas-Datasheet.pdf>> (25 January 2022 ).
- [11] “Laser Components IAG-Series.”, <<https://www.lasercomponents.com/uk/product/ingaas-apds-1100-1700-nm/>> (25 January 2022 ).
- [12] Shiyu Xie, Shiyong Zhang and Chee Hing Tan., “InGaAs/InAlAs Avalanche Photodiode With Low Dark Current for High-Speed Operation,” *IEEE Photonics Technol. Lett.* **27**(16), 1745–1748 (2015).
- [13] Campbell, J. C., Demiguel, S., Ma, F., Beck, A., Guo, X., Wang, S., Zheng, X., Li, X., Beck, J. D., Member, S., Kinch, M. A., Huntington, A., Coldren, L. A., Decobert, J. and Tschertner, N., “Recent Advances in Avalanche Photodiodes,” *IEEE J. Sel. Top. Quantum Electron.* **10**(6), 1446–1447 (2004).
- [14] “Optogration.”, <[http://www.optogration.com/apd\\_products.htm](http://www.optogration.com/apd_products.htm)> (25 January 2022 ).